

Thickness-dependent magnetic order and phase transition in V_5S_8

Rui-Zi Zhang(张瑞梓), Yu-Yang Zhang(张余洋), Shi-Xuan Du(杜世萱)

Citation: Chin. Phys. B . 2020, 29(7): 077504 . **doi:** 10.1088/1674-1056/ab8db1
Journal homepage: http://cpb.iphy.ac.cn; http://iopscience.iop.org/cpb

What follows is a list of articles you may be interested in

Double spin-glass-like behavior and antiferromagnetic superexchange interaction between Fe^{3+} ions in α-$Ga_{2-x}Fe_xO_3$ ($0 \le x \le 0.4$)

Lv Yi-Fei, Xiang Jian-Yong, Wen Fu-Sheng, Lv Wei-Ming, Hu Wen-Tao, Liu Zhong-Yuan

Chin. Phys. B . 2015, 24(3): 037502 . **doi:** 10.1088/1674-1056/24/3/037502

Exchange bias in ferromagnet/antiferromagnet bilayers

Shi Zhong, Du Jun, Zhou Shi-Ming

Chin. Phys. B . 2014, 23(2): 027503 . **doi:** 10.1088/1674-1056/23/2/027503

The variation of Mn-dopant distribution state with x and its effect on the magnetic coupling mechanism in $Zn_{1-x}Mn_xO$ nanocrystals

Cheng Yan, Hao Wei-Chang, Li Wen-Xian, Xu Huai-Zhe, Chen Rui, Dou Shi-Xue

Chin. Phys. B . 2013, 22(10): 107501 . **doi:** 10.1088/1674-1056/22/10/107501

Flexible tuning microwave permeability spectrum in $[ferromagnet/antiferromagnet]_n$ exchange-biasedmultilayer stack structure

Jin Li-Chuan, Zhang Huai-Wu, Tang Xiao-Li, Bai Fei-Ming, Zhong Zhi-Yong

Chin. Phys. B . 2013, 22(4): 047502 . **doi:** 10.1088/1674-1056/22/4/047502

The magnetic properties of diluted $CoFe_2O_4$ nanomaterials

R. Masrour,M. Hamedoun,A. Benyoussef

Chin. Phys. B . 2012, 21(4): 047501 . **doi:** 10.1088/1674-1056/21/4/047501

Thickness-dependent magnetic order and phase transition in V_5S_8*

Rui-Zi Zhang(张瑞梓)[1], Yu-Yang Zhang(张余洋)[1,2], and Shi-Xuan Du(杜世萱)[1,2,†]

[1] *Institute of Physics & University of Chinese Academy of Sciences, Chinese Academy of Sciences, Beijing* 100190, *China*
[2] *CAS Centre for Excellence in Topological Quantum Computation, Beijing* 100190, *China*

(Received 6 April 2020; revised manuscript received 24 April 2020; accepted manuscript online 28 April 2020)

V_5S_8 is an ideal candidate to explore the magnetism at the two-dimensional (2D) limit. A recent experiment has shown that the V_5S_8 thin films exhibit an antiferromagnetic (AFM) to ferromagnetic (FM) phase transition with reducing thickness. Here, for the first time, using density functional theory calculations, we report the antiferromagnetic order of bulk V_5S_8, which is consistent with the previous experiments. The specific antiferromagnetic order is reproduced when $U_{\rm eff} = 2$ eV is applied on the intercalated vanadium atoms within LDA. We find that the origin of the magnetic ordering is from superexchange interaction. We also investigate the thickness-dependent magnetic order in V_5S_8 thin films. It is found that there is an antiferromagnetic to ferromagnetic phase transition when V_5S_8 is thinned down to 2.2 nm. The main magnetic moments of the antiferromagnetic and ferromagnetic states of the thin films are located on the interlayered vanadium atoms, which is the same as that in the bulk. Meanwhile, the strain in the thin films also influences the AFM–FM phase transition. Our results not only reveal the magnetic order and origin in bulk V_5S_8 and thin films, but also provide a set of parameters which can be used in future calculations.

Keywords: V_5S_8, superexchange interaction, AFM–FM phase transition

PACS: 75.50.Ee, 75.30.Et, 73.43.Nq **DOI:** 10.1088/1674-1056/ab8db1

1. Introduction

Intrinsic magnetism in two-dimensional (2D) materials has been investigated extensively for years.[1–4] According to Mermin–Wagner theorem, the long-range magnetic order can hardly exist in the 2D regime due to the strong thermal fluctuations, while the magnetic anisotropy can overcome the thermal fluctuations.[5] In recent years, 2D ferromagnetic (FM) insulators, such as CrI_3 and $Cr_2Ge_2Te_6$,[6,7] and metallic ferromagnets, such as Fe_3GeTe_2,[8,9] have been synthesized in experiments. Meanwhile, various 2D materials are also expected to exhibit magnetic order in density functional theory (DFT) calculations.[10–15] In addition, the 2D magnets have been applied to fabricate various 2D heterostructures with engineered levels of strain, chemistry, optical, and electrical properties.[2,16–18] Hence, exploring the 2D magnets together with the material engineering could open up a wide range of possibilities for the fundamental physics and the design of spintronics devices.

The magnetic order of 2D magnets can be controlled by using external means, such as magnetic field[19] and current.[20,21] In many 2D magnets, the magnetic ordering exhibits thickness-dependent properties. Some 2D vdW magnets, such as CrI_3[22] and $MnBi_2Te_4$,[23] have been predicted to exhibit ferromagnetic ordering in monolayer while the thin films with even number of layers exhibit interlayer antiferromagnetic (AFM) ordering. In addition, the magnetic ordering in some thin films can be tuned in a process of a spin-reorientation transition (SRT), which is usually driven by thickness.[24–26] For example, reduction of the thickness of FeRh results in an antiferromagnetic to ferromagnetic phase transition.[25]

V_5S_8, which exhibits antiferromagnetism in bulk, also exhibits thickness-dependent properties in magnetic order. An AFM to FM phase transition is reported to occur when the thickness is down to 3.2 nm while a spin-glass-like state is found during the transition.[27] Meanwhile, the magnetoresistance hysteresis disappears as the thickness is reduced, suggesting that the metamagnetic transition changes from first order to second order.[28] Although the single-layer V_5S_8 has not been synthesized yet, the intriguing thickness-dependent magnetism accomplished with other magnetic properties makes V_5S_8 a candidate for future spin related applications. However, the question remains open on the mechanism of magnetism and the phase transition occurred in V_5S_8 films.

In this paper, we investigate the magnetic order of V_5S_8 bulk and thin films using DFT calculations. We find that the bulk V_5S_8 exhibits antiferromagnetism while only the intercalated vanadium atoms have magnetic moments, which is consistent with previous experiments. Our calculation results reveal that the magnetic exchange coupling is from superexchange interaction. Thickness-dependent magnetic order shows that the FM states become more stable with reducing thickness. The critical thickness of the AFM–FM transition

*Project supported by the National Natural Science Foundation of China (Grant Nos. 51922011 and 61888102), the National Key Research & Development Project of China (Grant Nos. 2016YFA0202300 and 2019YFA0308500), and the Strategic Priority Research Program of Chinese Academy of Sciences (Grant Nos. XDB30000000 and XDB28000000). A portion of the research was performed in CAS Key Laboratory of Vacuum Physics.

†Corresponding author. E-mail: sxdu@iphy.ac.cn

© 2020 Chinese Physical Society and IOP Publishing Ltd

ranges from 1.4 nm to 2.2 nm depending on different surface terminations. The major magnetism of the thin films originates from the same type of vanadium atoms, the interlayer vanadium, as that in the bulk material. However, the other types of vanadium atoms, those in the VS_2 layers, gradually exhibit small magnetic moments with reducing thickness. Meanwhile, the phase transition can also be affected by the strain in the thin films. Our results verify the existence of AFM to FM phase transition in V_5S_8 thin films and provide a possible mechanism for the AFM–FM phase transition.

2. Computational methods

All DFT calculations are performed using the Vienna *ab initio* simulation package (VASP).[29,30] The interactions between valence electrons and ionic cores are described with the projector augmented wave (PAW) method.[31,32] A plane wave basis set with a cutoff energy of 520 eV is used to expand the wave functions. For the exchange and correlation, we mainly employ the LDA+U approximation,[33] and compare the Perdew–Burke–Ernzerhof (PBE) functionals[34] with PBE+U. The atomic coordinates are fully optimized until the forces are smaller than 0.01 eV/Å. We use a vacuum spacing of 20 Å, which reduces the image interactions caused by the periodic boundary conditions. The Brillouin-zone integration is carried out using $2\times8\times4$ and $2\times8\times1$ Monkhorst–Pack k-point meshes for bulk and thin films V_5S_8, respectively. To treat the localized d orbitals of V atom, we use Dudarev's approach with the rotationally invariant effective U parameters $U_{\rm eff}=U-J$, where U and J are the on-site Coulomb and the exchange parameters, respectively.[35]

3. Results and discussion

Bulk V_5S_8 adopts a monoclinic structure with $F_{2/m}$ space group, as shown in Fig. 1(a).[36] The structure can be viewed as one layer of V atoms (red ones in Fig. 1) intercalated into VS_2 layers with 1T phase. Meanwhile, the intercalated V atoms lead to a distorted 1T-VS_2 layer. Therefore, there are three inequivalent V sites drawn in three different colors: V(1) (red), V(2) (blue), and V(3) (green). The intercalated V atoms are on the V(1) sites, forming a slightly distorted triangular lattice. The magnetic properties of bulk V_5S_8 have been investigated experimentally for decades.[37–39] It has an antiferromagnetic ground state while the critical temperature is around 32 K. Neutron scattering[40] and nuclear magnetic resonance[41] experiments revealed that the intercalated V atoms are responsible for the magnetism. The antiferromagnetic alignment of spins is depicted in Fig. 1(b) according to previous reports.[40] Despite experimental investigations, few theoretical works have been reported.

First, we try to reproduce the generally accepted magnetic ordering of bulk V_5S_8, AFM ground state with the magnetism from intercalated V(1) atoms, using DFT based quantum mechanical calculations by comparing the total energy between the configurations with different magnetic orderings. Here, we construct three different types of AFM states and one FM state among which AFM-1 has been generally accepted based on experimental observations, as shown in Figs. 1(b)–1(e). The energy difference is defined as $\Delta E=E_{{\rm AFM}-n}-E_{\rm FM}$, where $E_{{\rm AFM}-n}$ and $E_{\rm FM}$ represent the total energies of AFM-n ($n=1$, 2, and 3) and FM structures, respectively. Negative ΔE means AFM state is more stable than FM state, vice versa. Meanwhile, we extract the magnetic moments on different V atoms for the AFM-1 structures to see if the magnetic moments only reside on the V(1) atoms. Here, the magnetic moment is neglected if it is smaller than 0.1 $\mu_{\rm B}$ due to the limitation of calculation precision.

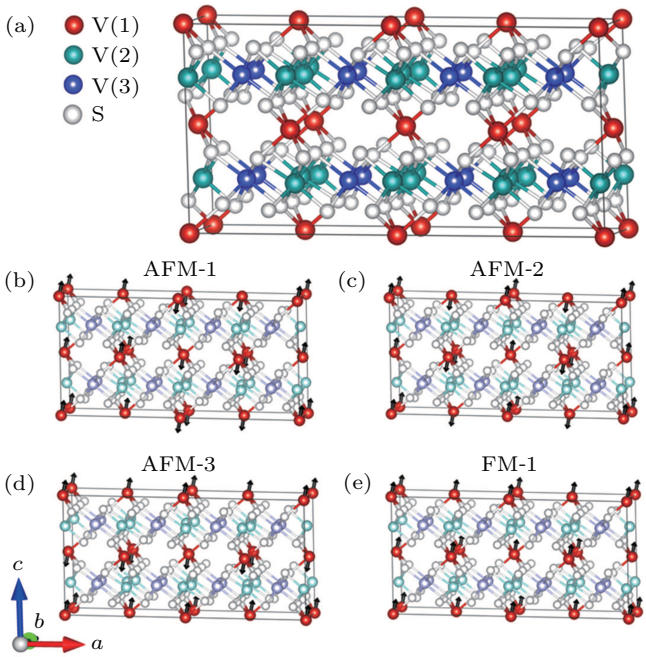


Fig. 1. Structures and magnetic order of bulk V_5S_8. (a) The crystal structure of V_5S_8. V(1), V(2), and V(3) represent the inequivalent V atoms. Various magnetic orders considered in our calculation: (b) AFM-1, (c) AFM-2, and (d) AFM-3 are three different types of AFM magnetic orders and (e) FM is the one possible FM magnetic order. Especially, AFM-1 is the magnetic order of bulk V_5S_8 determined by the neutron diffraction measurements.[40]

In order to obtain the correct ground state of bulk V_5S_8, AFM-1, we perform the calculations on the four configurations shown in Fig. 1 with different effective interaction parameters ($U_{\rm eff}$) and different exchange correlation functionals. $U_{\rm eff}$ has been applied on all vanadium atoms in the initial states. The exchange–correlation functionals we used are LDA and PBE. The ΔEs calculated with LDA and PBE are presented in the upper panels of Figs. 2(a) and 2(b), respectively. The calculations with LDA function show that the AFM-2 state is the most stable state and the energy difference between AFM-1 and AFM-2 is less than 0.2 eV using different $U_{\rm eff}$. The calculations with PBE functional find that

the AFM-1 state is the most state. Therefore, both functionals show reasonable results and the PBE functional is a little bit better from the view of total energy. Then, we check the magnetic moments on different vanadium atoms for the AFM-1 state using LDA and PBE functionals, which are shown in the lower panels of Figs. 2(a) and 2(b), respectively. Both V(2) and V(3) atoms have nonnegligible magnetic moments for the PBE functional. As for LDA, though some of the V(2) atoms have a nonnegligible magnetic moment, $0.11 \pm 0.07\ \mu_B$ in average, the magnetic moment of the V(3) atoms are tiny. Since previous experiments[38] reported that only V(1) atoms are responsible for the magnetism, it seems that $U_{\rm eff}$ employed on all the vanadium atoms in the initial state cannot generate the correct antiferromagnetic ground state. We then employ $U_{\rm eff}$ on the V(1) atoms only. The variations of ΔEs and the average magnetic moments with different $U_{\rm eff}$s ranging from 0.5 to 4.0 are shown in Figs. 2(c) and 2(d) for LDA and PBE functionals, respectively. For the LDA+U calculations, the FM state is the ground state when $U_{\rm eff}$ is smaller than 2 eV with negligible magnetic contribution from the V(2) and V(3) atoms (the magnetic moments of both V(2) and V(3) atoms are less than 0.1 μ_B). The AFM-1 state becomes the ground state if $U_{\rm eff}$ is equal to 2 eV while the AFM-2 state becomes the ground state if $U_{\rm eff}$ is larger than 2 eV. For PBE+U, the AFM-3 state is always energy favorable for different $U_{\rm eff}$s. Based on the above calculations, we find that DFT calculations with $U_{\rm eff}$ less than 2 eV for V(1) atoms within LDA generate a ground state which agrees well with experimental observations. Therefore, we do further calculations within the LDA+U formalism using $U_{\rm eff} = 2$ eV for the V(1) atoms only.

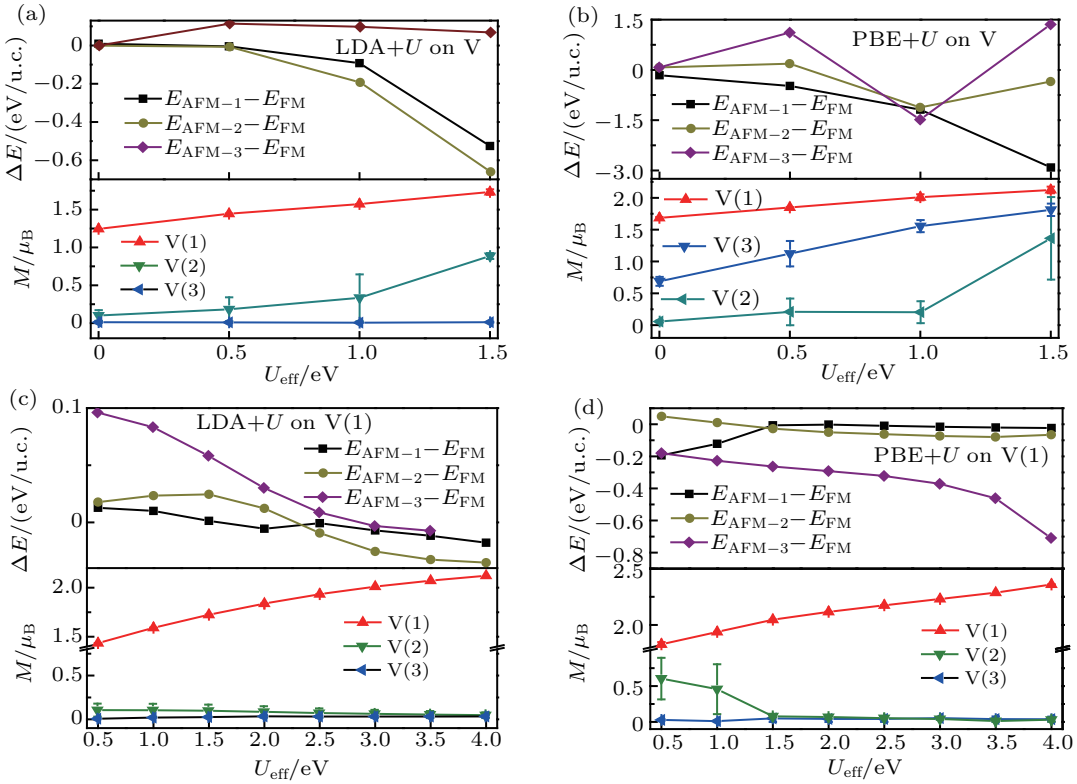


Fig. 2. The energy difference ΔE (upper panel) and the average magnetic moments of V(1), V(2), and V(3) atoms in AFM-1 structure as a function of $U_{\rm eff}$. (a) LDA+U and (b) PBE+U with varied $U_{\rm eff}$ from 0 to 1.5 on all V atoms. (c) LDA+U and (d) PBE+U with varied $U_{\rm eff}$ from 0 to 4 on V(1) atoms only.

According to the crystal structure, the distance between two V(1) atoms is around 6.5 Å. How the cooperative magnetism occurs in such large distance still remains unclear. The distance between two V(1) atoms is too large for direct coupling. In general, the indirect magnetic coupling can be distinguished into superexchange interaction and RKKY interaction.[42] The superexchange interaction is controlled by a shared ligand of metals.[43,44] Changing the angle between the metals and ligand will affect the metal–ligand orbital overlap and the subsequent superexchange. While, the nature of RKKY is determined by the density of conduction electrons and the metal–metal distance.[43,45] Therefore, the exchange coupling can be RKKY interaction if it is very sensitive to the distance or can be superexchange if it is sensitive to the angle between the metals and ligand.

To investigate the indirect V(1)–V(1) magnetic coupling, we evaluate and compare the total energies of 4 magnetic orderings mentioned above. The distance effects are exhibited by expanding each lattice constant for 1% to 3%. The energy differences are shown in Fig. 3(a). The AFM-1 structure is always energy favorable. This indicates that the V(1)–V(1) coupling is not sensitive to the distance, which means RKKY in-

teraction does not contribute to the magnetic ordering. Meanwhile, we move the V(1) atom along *a*-axis and *c*-axis for 1% of lattice constant to change the angle between V(1) atoms and VS_2 layer, as shown in Fig. 3(b). The AFM-2 structure is more stable than the AFM-1 structure with the movement of V(1) atom along the *a*-axis. The FM structure becomes the ground state if the V(1) atoms move along the *c*-axis. This indicates that the V(1)–V(1) coupling changes if the angle between ligand VS_2 and metal V(1) is changed. Hence, the superexchange interaction results in the magnetic ordering of V_5S_8.

To understand the physical nature of the thickness-driven AFM to FM phase transition observed in experiments,[27] we perform calculations of the magnetic order in V_5S_8 thin films. Since V_5S_8 can be regarded as the VS_2 intercalated with V(1) atoms, there are three types of thin films with different terminations as defined in Fig. 4(a): V(1)–V(1), V(1)–VS_2, and VS_2–VS_2 terminated monolayers.

Here, we use the energy difference, $\Delta E = E_{\mathrm{AFM-1}} - E_{\mathrm{FM}}$, to depict the phase transition with different thicknesses. As shown in Fig. 4(b), the ΔE turns to positive from negative with the decrease of the thickness, suggesting that the FM state becomes the ground state instead of AFM state. The transition from AFM state to FM agrees with previous experimental observation.[27] Meanwhile, the AFM–FM phase transition is independent of the terminated surfaces and occurs on all the three types of thin films at different thicknesses. From Fig. 4(c), we find that the V(1) atoms contribute the most magnetism in the thin films we considered, which is independent of the thicknesses. However, the magnetic moments vary from the bulk due to different external environment. Particularly, the internal V(1) atoms generate a magnetic moment around 1.8 μ_B, while the V(1) atoms on the surface generate a magnetic moment around 2.5 μ_B. Meanwhile, some of the V(2) and V(3) atoms also reserve magnetic moments in the thin films.

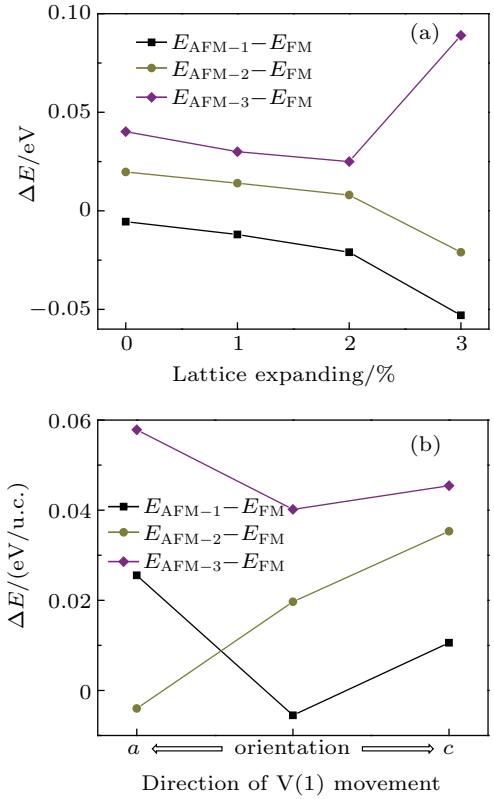


Fig. 3. The energy difference (ΔE) of different AFM states as a function of (a) lattice expanding and (b) the movement of V(1) atom along different directions.

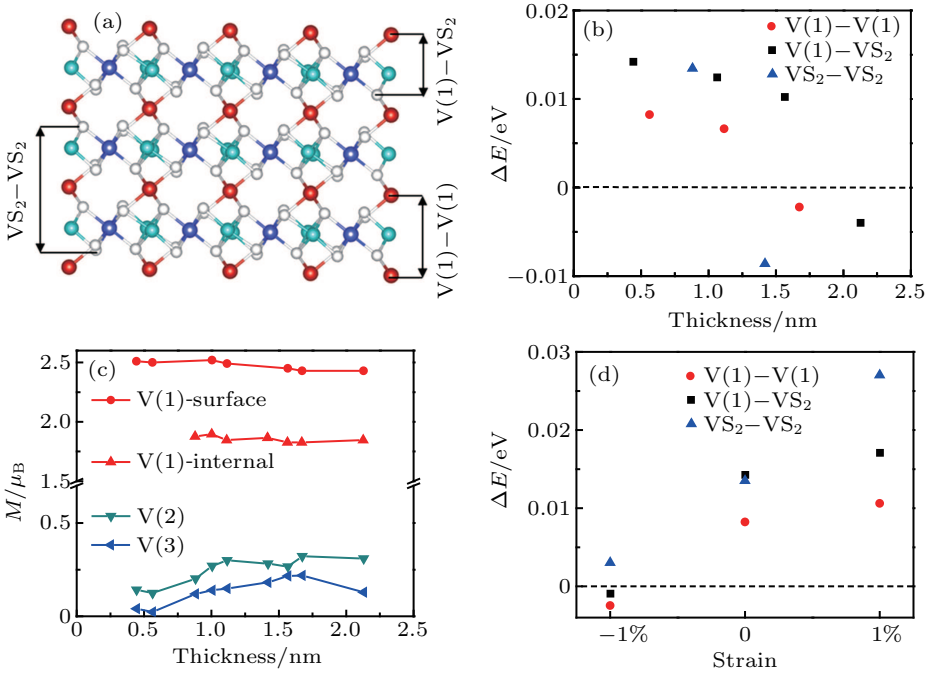


Fig. 4. (a) The schematic of monolayer in V_5S_8 thin films with V(1)–V(1), VS_2–V(1), and VS_2–VS_2 terminations. (b) The ΔEs at different thicknesses. (c) The magnetic moments of V(1), V(2), and V(3) at different thicknesses. (d) The ΔEs of monolayers with all three types of terminations as a function of the strain.

In our calculation, the phase transition occurs at a thickness ranging from 1.4 nm to 2.2 nm, while the experiment discovered the phase transition at a thickness around 3 nm. To understand the thickness difference between our calculation and the experiments, we do further calculations on the thin films under strain since the strain influences the magnetism in many materials.[25,46] The strain is induced by expanding or compressing the lattice constant. Here, we only consider monolayers of the three types of thin films to explore the effect of the strain. For all three types of monolayers, the ΔEs (Fig. 4(d)) decrease after 1% compression of the lattice constant and increase after 1% expansion. For V(1)–V(1) and V(1)–VS_2 monolayers, the AFM-1 state even becomes the stable state after the compression. Hence, the strain can influence the AFM–FM phase transition in the V_5S_8 films. In the experiments, the thin films can be introduced with strain due to the thermal expansion accomplished with the change of temperature or the substrate. However, our model is based on an ideal external environment. Hence, the thickness that induced the phase transition can be different between calculations and experiments.

4. Conclusion

In summary, we investigate the magnetic order of V_5S_8 in bulk and thin films using DFT calculations. We find that the bulk V_5S_8 exhibits antiferromagnetism while only V(1) atoms are responsible for the magnetism, which is consistent with previous experiments. The specific parameters ($U_{\text{eff}} = 2$ eV applied on the intercalated vanadium atoms within LDA functional) can reproduce the antiferromagnetic order, which is consistent with experiments. We discover that the magnetic ordering originates from superexchange interaction. In the V_5S_8 thin films, the AFM to FM phase transition occurs at a thickness ranging from 1.4 nm to 2.2 nm and the FM state, which is contributed by V(1) atom, becomes more stable with reducing thickness. Our results provide a set of parameters used in calculations that result in the magnetic ordering reported by the experiment for V_5S_8 bulk materials. Furthermore, our calculations based on these parameters show a thickness dependent AFM–FM transition that agrees with the experimental observations.

References

[1] Burch K S, Mandrus D and Park J G 2018 *Nature* **563** 47
[2] Gong C and Zhang X 2019 *Science* **363** eaav4450
[3] Seyler K L, Zhong D, Klein D R, Gao S, Zhang X, Huang B, Navarro-Moratalla E, Yang L, Cobden D H, McGuire M A, Yao W, Xiao D, Jarillo-Herrero P and Xu X 2018 *Nat. Phys.* **14** 277
[4] Bonilla M, Kolekar S, Ma Y, Diaz H C, Kalappattil V, Das R, Eggers T, Gutierrez H R, Phan M H and Batzill M 2018 *Nat. Nanotechnol.* **13** 289
[5] Mermin N D and Wagner H 1966 *Phys. Rev. Lett.* **17** 1133
[6] Gong C, Li L, Li Z, Ji H, Stern A, Xia Y, Cao T, Bao W, Wang C, Wang Y, Qiu Z Q, Cava R J, Louie S G, Xia J and Zhang X 2017 *Nature* **546** 265
[7] Huang B, Clark G, Navarro-Moratalla E, Klein D R, Cheng R, Seyler K L, Zhong D, Schmidgall E, McGuire M A, Cobden D H, Yao W, Xiao D, Jarillo-Herrero P and Xu X 2017 *Nature* **546** 270
[8] Fei Z, Huang B, Malinowski P, Wang W, Song T, Sanchez J, Yao W, Xiao D, Zhu X, May A F, Wu W, Cobden D H, Chu J H and Xu X 2018 *Nat. Mater.* **17** 778
[9] Deng Y, Yu Y, Song Y, Zhang J, Wang N Z, Sun Z, Yi Y, Wu Y Z, Wu S, Zhu J, Wang J, Chen X H and Zhang Y 2018 *Nature* **563** 94
[10] O'Hara D J, Zhu T, Trout A H, Ahmed A S, Luo Y K, Lee C H, Brenner M R, Rajan S, Gupta J A, McComb D W and Kawakami R K 2018 *Nano Lett.* **18** 3125
[11] Zhuang H L and Hennig R G 2016 *Phys. Rev. B* **93** 054429
[12] You J Y, Zhang Z, Gu B and Su G 2019 *Phys. Rev. Appl.* **12** 024063
[13] Dong X J, You J Y, Gu B and Su G 2019 *Phys. Rev. Appl.* **12** 014020
[14] Yin K, Zhang Y Y, Zhou Y, Sun L, Chisholm M F, Pantelides S T and Zhou W 2016 *2D Mater.* **4** 011001
[15] Pan L, Wen H, Huang L, Chen L, Deng H X, Xia J B and Wei Z 2019 *Chin. Phy. B* **28** 107504
[16] Hagmann J A, Li X, Chowdhury S, Dong S N, Rouvimov S, Pookpanratana S J, Man Yu K, Orlova T A, Bolin T B, Segre C U, Seiler D G, Richter C A, Liu X, Dobrowolska M and Furdyna J K 2017 *New J. Phys.* **19** 085002
[17] Gibertini M, Koperski M, Morpurgo A F and Novoselov K S 2019 *Nat. Nanotechnol.* **14** 408
[18] Yuan X Y, Xue X B, Si L F, Du J and Xu Q Y 2012 *Chin. Phys. Lett.* **29** 097701
[19] Huang B, Clark G, Klein D R, MacNeill D, Navarro-Moratalla E, Seyler K L, Wilson N, McGuire M A, Cobden D H, Xiao D, Yao W, Jarillo-Herrero P and Xu X 2018 *Nat. Nanotech.* **13** 544
[20] Chen X Z, Liu H, Yin L F, Song C, Tan Y Z, Zhou X F, Li F, You Y F, Sun Y M and Pan F 2019 *Phys. Rev. Appl.* **11** 024021
[21] Guo X, Li D and Xi L 2018 *Chin. Phys. B* **27** 097506
[22] Sivadas N, Okamoto S, Xu X, Fennie C J and Xiao D 2018 *Nano Lett.* **18** 7658
[23] Otrokov M M, Rusinov I P, Blanco-Rey M, Hoffmann M, Vyazovskaya A Y, Eremeev S V, Ernst A, Echenique P M, Arnau A and Chulkov E V 2019 *Phys. Rev. Lett.* **122** 107202
[24] Oepen H P, Speckmann M, Millev Y and Kirschner J 1997 *Phys. Rev. B* **55** 2752
[25] Yu C Q, Li H, Luo Y M, Zhu L Y, Qian Z H and Zhou T J 2019 *Phys. Lett. A* **383** 2424
[26] Kouvel J S and Hartelius C C 1962 *J. Appl. Phys.* **33** 1343
[27] Niu J, Yan B, Ji Q, Liu Z, Li M, Gao P, Zhang Y, Yu D and Wu X 2017 *Phys. Rev. B* **96** 075402
[28] Hardy W J, Yuan J, Guo H, Zhou P, Lou J and Natelson D 2016 *ACS Nano* **10** 5941
[29] Kresse G 1995 *J. Non-Cryst. Solids* **192–193** 222
[30] Kresse G and Furthmuller J 1996 *Phys. Rev. B* **54** 11169
[31] Blochl P E 1994 *Phys. Rev. B* **50** 17953
[32] Kresse G and Joubert D 1999 *Phys. Rev. B* **59** 1758
[33] Anisimov V I, Zaanen J and Andersen O K 1991 *Phys. Rev. B* **44** 943
[34] Perdew J P, Burke K and Ernzerhof M 1996 *Phys. Rev. Lett.* **77** 3865
[35] Dudarev S L, Botton G A, Savrasov S Y, Humphreys C J and Sutton A P 1998 *Phys. Rev. B* **57** 1505
[36] Kawada I, Nakanoonoda M, Ishii M, Saeki M and Nakahira M 1975 *J. Solid State Chem.* **15** 246
[37] Nakanishi M, Yoshimura K, Kosuge K, Goto T, Fujii T and Takada J 2000 *J. Magn. Magn. Mater.* **221** 301
[38] Nozaki H, Umehara M, Ishizawa Y and Saeki M 1978 *J. Phys. Chem. Solids* **39** 851
[39] Nozaki H and Ishizawa Y 1977 *Phys. Lett. A* **63** 131
[40] Funahashi S, Nozaki H and Kawada I 1981 *J. Phys. Chem. Solids* **42** 1009
[41] Silbernagel B G, Levy R B and Gamble F R 1975 *Phys. Rev. B* **11** 4563
[42] Hurd C M 1982 *Contemp. Phys.* **23** 469
[43] Zhang Y and Miller G J 2015 *J. Phys. Chem. C* **119** 580
[44] Zhu M, Do D, Dela Cruz C R, Dun Z, Cheng J G, Goto H, Uwatoko Y, Zou T, Zhou H D, Mahanti S D and Ke X 2015 *Phys. Rev. B* **92** 094419
[45] Yao J, Zhang Y, Wang P L, Lutz L, Miller G J and Mozharivskyj Y 2013 *Phys. Rev. Lett.* **110** 077204
[46] Xie Y, Feng J, Xiang H and Gong X 2019 *Chin. Phys. Lett.* **36** 056801